Electrochimica Acta 89 (2013) 284–291

Contents lists available at SciVerse ScienceDirect

Electrochimica Acta

journal homepage: www.elsevier.com/locate/electacta

Electrodeposition for preparation of efficient surface-enhanced Raman scattering-active silver nanoparticle substrates for neurotransmitter detection

Marta Siek, Agnieszka Kaminska**, Anna Kelm, Tomasz Rolinski, Robert Holyst, Marcin Opallo[1], Joanna Niedziolka-Jonsson*,[1]

Institute of Physical Chemistry, Polish Academy of Sciences, 44/52 Kasprzaka, 01-224 Warsaw, Poland

ARTICLE INFO

Article history:
Received 18 September 2012
Received in revised form 5 November 2012
Accepted 6 November 2012
Available online 21 November 2012

Keywords:
Electrodeposition
Silver nanoparticles
SERS-active surfaces
Neurotransmitters
Choline

ABSTRACT

A stable and efficient surface-enhanced Raman scattering (SERS) substrate for neurotransmitter and cholinergic neurotransmission precursor detection was obtained by silver nanoparticle (AgNP) electrodeposition onto tin-doped indium oxide (ITO) using cyclic voltammetry. The size and surface coverage of the deposited AgNPs were controlled by changing the scan rate and the number of scans. The SERS performance of these substrates was analyzed by studying its reproducibility, repeatability and signal enhancement measured from p-aminothiophenol (p-ATP) covalently bonded to the substrate. We compared the SERS performance for samples with different Ag particle coverage and particle sizes. The performance was also compared with a commercial substrate. Our substrates exhibited a SERS enhancement factor of around 10^7 for p-ATP which is three orders of magnitude larger than for the commercial substrate. Apart from this high enhancement effect the substrate also shows extremely good reproducibility. The average spectral correlation coefficient (Γ) is 0.96. This is larger than for the commercial substrate (0.85) exhibiting a much lower SERS signal intensity. Finally, the application of our substrates as SERS bio-sensors was demonstrated with the detection of the neurotransmitters acetylcholine, dopamine, epinephrine and choline, the precursor for acetylcholine. The intensive SERS spectra observed for low concentrations of choline (2×10^{-6} M), acetylcholine (4×10^{-6} M), dopamine (1×10^{-7} M) and epinephrine (7×10^{-4} M) demonstrated the high sensitivity of our substrate. The high sensitivity and fast data acquisition make our substrates suitable for testing physiological samples.

1. Introduction

Since the initial discovery of surface-enhancement of Raman scattering on roughened silver electrode surfaces [1,2] researchers have explored numerous promising substrates that can be used as efficient surface-enhanced Raman scattering (SERS) platforms [3–10]. Recently special interest has been devoted to nanosized Ag particles (AgNPs) as SERS substrates because they strongly scatter light and their optical properties depend on their size, shape and aggregation state [11,12]. Although considerable progress has been made towards improving and optimizing SERS substrates for analytical applications [13–15], the fabrication of high-throughput, low-cost and reproducible SERS platforms still remains a challenging task.

In practice the creation of SERS substrates is often a trade-off between sensitivity, reproducibility, stability, ease and cost of production. An enormous enhancement of 10^{14} was reported for specially screened colloidal silver particles [16–20]. The most reproducible SERS substrates are prepared by etching optical fibres in HF and covering them in silver. The relative standard deviation (RSD) for a single sample is less than 2% [21]. However, none of these methods is suitable for larger scale production. High throughput methods such as etching, evaporation, screen printing and electrodeposition generally show reasonable enhancement and a RSD in the range of 5–30% [22–27]. Substrates obtained by methods based on physical vapor deposition often suffer from being quite fragile; the SERS-active particles are easily removed from the surface and additional protective layers might be necessary which reduces the SERS sensitivity [28]. This can be overcome by screen printing [27] or by electrochemical methods where the particles are directly electrodeposited onto the surface. Numerous protocols describing electrochemical methods of silver nanostructure preparation for SERS applications have been published. These include galvanostatic methods [29,30], double-potentiostatic electrodeposition [31,32], templated deposition in a membrane [33,34] and cyclic voltammetry where the influence of

* Corresponding author. Tel.: +48 22 343 32 59; fax: +48 22 343 33 33.
** Corresponding author. Tel.: +48 22 343 32 28; fax: +48 22 343 33 33.
E-mail addresses: akamin@ichf.edu.pl (A. Kaminska), joaniek@ichf.edu.pl (J. Niedziolka-Jonsson).
[1] ISE member.

0013-4686/$ – see front matter © 2012 Elsevier Ltd. All rights reserved.
http://dx.doi.org/10.1016/j.electacta.2012.11.037

the applied potentials and addition of complexing agents [35] were investigated.

An important goal, both from an environmental and economic point of view is avoiding harmful chemicals. Many chemical and electrochemical methods involve the usage of hazardous compounds such as potassium cyanide [36] or sodium borohydride [37].

In the present work we demonstrate a facile, rapid, harmless and low-cost electrochemical method for deposition of silver nanoparticles (AgNPs) to create a mechanically and chemically durable SERS platform with good enhancement and excellent signal reproducibility. The AgNPs are electrodeposited onto tin-doped indium oxide (ITO) in the presence of citrate [29–32] using cyclic voltammetry. This is similar to reports recently presented using galvanostatic [29,30] and double-potentiostatic electrodeposition [31,32]. The structure and the surface morphology of the Ag nanoparticulate films are characterized by scanning electron microscopy (SEM), atomic force microscopy (AFM), and UV–vis spectroscopy. The density and size of the AgNPs can be tuned by varying the scan rate and the number of scans. We measure the SERS enhancement as a function of the deposited particle properties and show that the resultant Ag-nanoparticle films exhibit very strong surface-enhancement effects which can be used in the design of efficient, stable SERS-active substrates for analytical applications. To exemplify this we show the detection of the neurotransmitters acetylcholine, dopamine, epinephrine and choline (a cholinergic neurotransmission precursor). Neurotransmitters play a crucial role for life and are for example responsible for much of the stimulation of muscles (acetylcholine) and reward mechanisms in the brain (dopamine). The concentration of neurotransmitters in the human body are associated with some diseases like schizophrenia or Parkinson's disease in the case of lack of dopamine [38] or Alzheimer's, where significant drop of acetylcholine concentration occurs in the brain. SERS is one among several different experimental techniques being developed for fast and accurate detection of low concentrations of neurotransmitters. Presently SERS spectra of neurotransmitters have been measured on colloidal silver nanoparticles [39], silver rough electrodes [40] and polymer-coated silver electrodes [41]. To the best of our knowledge, we present here the first SERS spectra of the cholinergic neurotransmission precursor choline.

2. Experimental

Silver nitrate ($AgNO_3$) and trisodium citrate dihydrate were purchased from POCH, p-aminothiophenol (p-ATP, 98%), choline chloride (98%), acetylcholine chloride (99%), dopamine hydrochloride and epinephrine (95%) were from Sigma–Aldrich, ethanol was from Chempur. ITO coated glass (resistivity 8–12 Ω/square) was from Delta Technologies. Water was purified with an ELIX system (Millipore). All reagents were used as received without further purification. The ITO electrodes were cleaned with ethanol, deionised water and finally heated for 10 min in a furnace at 500 °C in air. Next, the ITO electrode surfaces were defined by masking with scotch tape. The electrodeposition of AgNPs was performed in an electrochemical cell consisting of three electrodes, ITO (geometric area 0.2 cm^2), platinum mesh and Ag wire (d = 0.5 mm) as the working, counter and quasi-reference electrodes, respectively. The electrodes were immersed into a deaerated aqueous solution of 0.25 mM of $AgNO_3$ and 0.25 mM sodium citrate. Cyclic voltammetry was done with an Autolab (Metrohm Autolab) electrochemical system with GPES software from 0 to −0.8 V with different scan rates of 5, 10 or 100 mV/s. After electrodeposition the electrodes were rinsed with deionised water, ethanol and dried under a stream of air. Scanning electron microscopy (SEM) images were taken with

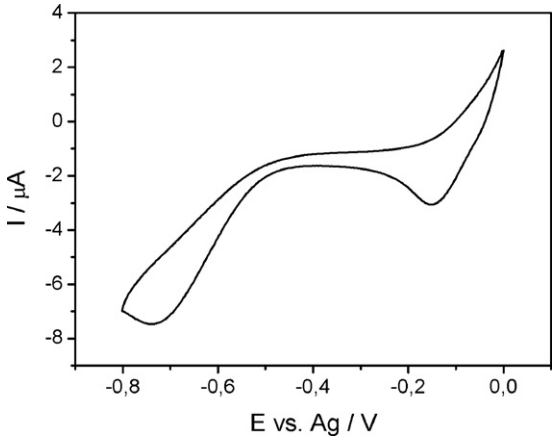

Fig. 1. Cyclic voltammetry of 0.25 mM $AgNO_3$ and 0.25 mM sodium citrate in water.

a Zeiss Supra scanning electron microscope. UV–vis spectra were collected with Thermo Evolution 300 spectrophotometer. The surface coverage and the diameter of the deposited nanoparticles in Fig. 1 were measured from SEM images using the ImageJ software. SERS measurements were carried out on dried samples using a Renishaw inVia Raman system equipped with a HeNe laser and a 300 mW diode laser emitting at 785 nm. The diode or the 632.8 nm HeNe line was used as the excitation source. The light from the laser was passed through a line filter, and focused on a sample mounted on an X–Y–Z translation stage with a 20× microscope objective. The Raman scattered light was collected by the same objective through a holographic notch filter to block out Rayleigh scattering. A 1800 groove/mm grating was used to provide a spectral resolution of 5 cm^{-1}. The Raman scattering signal was recorded by a 1024 × 256 pixel RenCam CCD detector. The beam diameter was approximately 5 μm. Typically, the normal Raman spectra were acquired for 20 min; for SERS experiments the spectra were acquired for 10–90 s with the laser power measured at the sample being 5 mW. When presenting the results, the spectra have been normalized by the laser power and the collection times. The enhancement factors of the various morphologically different substrates were quantified and compared using p-aminothiophenol. p-ATP was chosen because it forms a highly repeatable and well-defined self-assembled monolayer with well-characterized Raman and SERS spectra. For controlling the reproducibility spectra were collected from five different samples from different batches. On each sample Raman spectra were collected from a 20 μm × 20 μm map and on each sample mapping was performed on at least 35 different positions. Prior to performing the reproducibility analysis all SERS spectra were processed with a Savitzky–Golay second derivative smoothing (window size of 39 data points with second order polynomial). The correlation coefficients between all non-identical spectral pairs ($i \neq j$) in the same data set were determined from the equation [42]

$$P_{i,j} = \frac{\sum_{k=1}^{W}(I_i(k) - \overline{I}_i)(I_j(k) - \overline{I}_j)}{\sigma_i \sigma_j} \quad (1)$$

where i and j are the index of the spectra in the data matrix, k is the wave number index of the individual spectra, I is the spectral intensity, W is the spectral range, and σ_i is the standard deviation of the spectrum. Once the correlation coefficients $P_{i,j}$ are calculated, Γ, the average of the off-diagonal correlation coefficients, can then be determined:

$$\Gamma \equiv \frac{2\sum_{i=1}^{N}\sum_{j=i+1}^{N} P_{ij}}{N(N-1)} \quad (2)$$

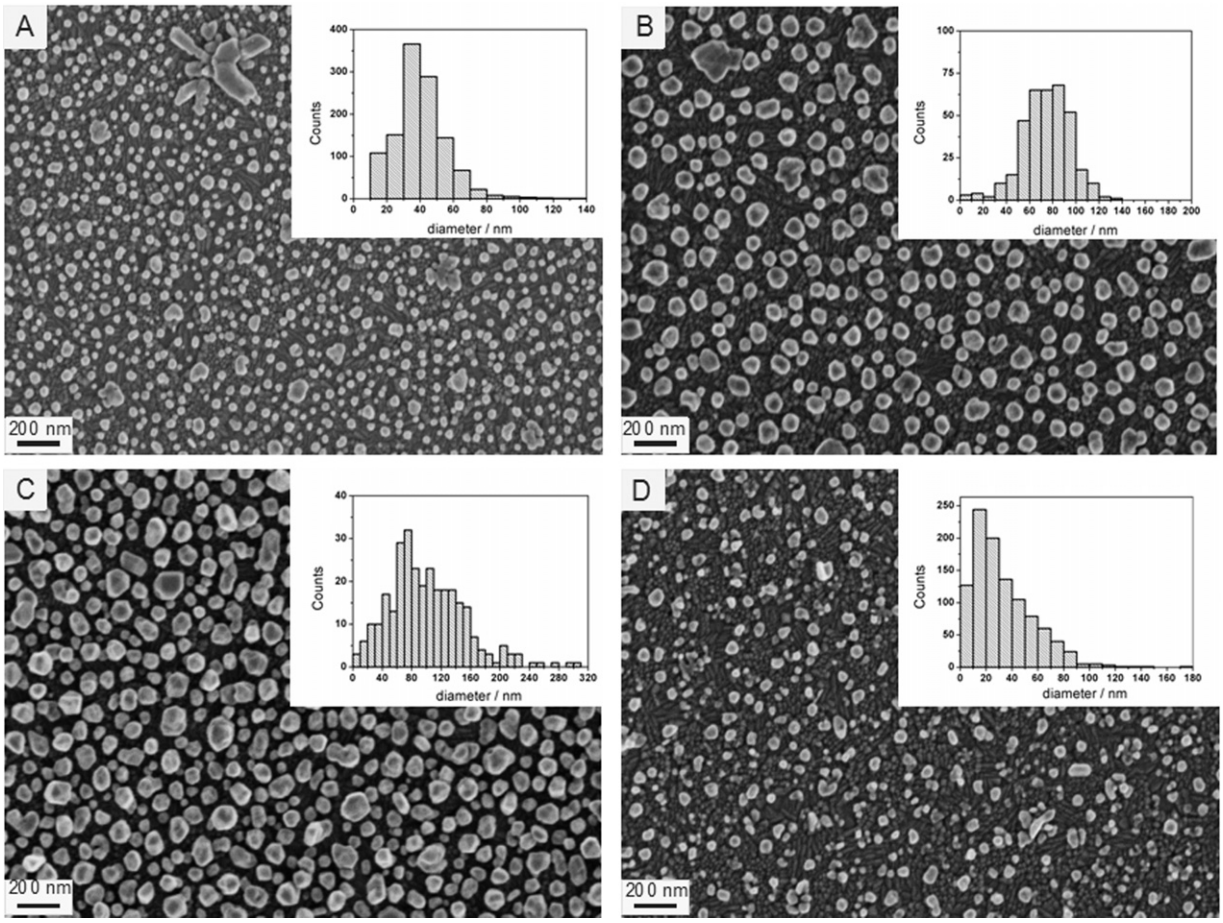

Fig. 2. SEM images of AgNPs deposited on the ITO surface with different scan rate: (A) 5 scans with 5 mV/s, (B) 20 scans with 10 mV/s, (C) 50 scans with 10 mV/s and (D) 50 scans with 100 mV/s. On insets histograms of particle diameter are presented.

Γ thus defined is an easily determined and very useful parameter for quantitative assessment of spectral reproducibility. Γ varies between 0 and 1, where 1 is the case of identical spectra and 0 the case of completely uncorrelated spectra. Γ as defined in Eq. (2) was used to estimate the reproducibility of multiple measurements.

3. Results and discussion

3.1. Preparation and surface characterization

For AgNP preparation cyclic voltammetry (CV) was used. Electrodeposition of Ag involves a single electron transfer reaction between the silver ion and the electrode. To enhance the efficiency of the electrode process a small amount of a chemical reducing agent (0.25 mM sodium citrate) was added [43]. At first different potential windows were tested and the degree of surface coverage was taken as an evaluation criterion for further investigation. A peak from the silver deposition appears at −0.08 V. If the scan direction is reversed just after the reduction peak a dense cover of particles is formed on the electrode. However, the size and morphology of the particles are very diverse, from small crystallites to large star-shaped structures. When the scan range was extended to −0.8 V a uniform and dense coverage was achieved. In Fig. 1 a typical CV from the extended scan range is shown with two peaks appearing: the Ag-deposition peak at −0.08 V and a peak at −0.66 V from oxygen reduction on the deposited particles. The shift of the switching potential to more negative values clearly affects the rate of the nucleation process [44].

The morphologies of the electrodeposited AgNP SERS substrates were monitored by SEM, and representative images are presented in Fig. 2. One can easily distinguish the influence of the scan rate on the particle size. The diameter increase together with increasing the scan rate and is in the range of 20–60 nm at 5 mV/s and between 50 and 100 nm at 10 mV/s. When the scan rate is increased further, to 100 mV/s the particle deposition is quite sparse. Increasing the number of scans at a fixed scan rate results in a denser coverage and somewhat larger particles. A systematic study of varying the scan rate and number of scans was performed, and SERS measurements were performed on each sample. Four samples showing promising SERS enhancement factors were chosen for further studies. Samples with these settings were produced in large numbers for more thorough SERS investigation. Fig. 2 shows representative SEM images of these samples.

Experiments were also performed without added citrate and the resulting particle deposit is sparse with larger particles with a wider diameter distribution. It seems that citrates are responsible for the uniform AgNP deposition on the surface [32].

3.2. Substrate optimalization for SERS

To gain insight into the dependence of the SERS enhancement on the size and density of the AgNPs SERS spectra of p-aminothiophenol (p-ATP) adsorbed onto the different patterned AgNPs film were recorded. These are shown in Fig. 3. The inset in Fig. 3 shows the Raman spectrum of solid p-ATP and SERS spectra (A–D) of p-ATP molecules adsorbed from 10^{-6} M aqueous solution onto the four surfaces presented in Fig. 2A–D, respectively.

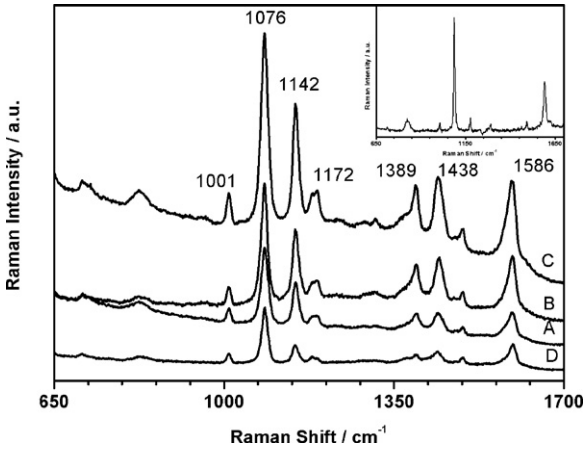

Fig. 3. SERS spectra of p-ATP recorded from four morphologically different surfaces from Fig. 2, A–D, respectively. Laser = 632.8 nm, power = 5 mW, integration time = 10 s. Inset shows the normal Raman spectrum of solid p-ATP. Laser = 632.8 nm, power = 60 mW, integration time = 60 s.

Compared to the normal Raman spectrum, marked changes in frequency shifts and relative intensity occurs for most of the bands in the SERS spectrum. On the basis of well-documented solid data [45] the bands at 1586, 1172, and 1076 cm^{-1} can be assigned to the vibration of the ν_{CC}, 8a (a_1), δ_{CH}, 9a (a_1) and ν_{CS}, 7a (a_1), respectively. The ν_{CS} vibration shifts from 1088 cm^{-1} (in inset in Fig. 3) to 1076 cm^{-1} in the SERS spectra (Fig. 3A–D), suggesting that the thiol group is directly bonded to the Ag surface. The peaks at 1438, 1389, and 1142 cm^{-1}, attributed respectively to the $19b_2$, $3b_2$, and $9b_2$ modes of p-ATP, are invisibly weak in the normal Raman spectrum, whereas they are comparable in intensity with the dominant band at 1076 cm^{-1} in the surface enhanced spectra. The enhancement mechanism for the a_1 modes is believed to be different from that of the b_2 modes. The enhancement of the b_2 modes has been ascribed to the charge transfer (CT) between the metal and the adsorbed molecules [46,47].

3.3. Enhancement factor determination

To estimate the enhancement ability of the AgNPs film, the surface enhancement factor (EF) was calculated according to the formula:

$$EF = \frac{I_{SERS} N_{NR}}{I_{NR} N_{SERS}} \quad (3)$$

where N_{SERS} and N_{NR} refers to the number of molecules adsorbed on the SERS probe within the laser spot area and the number of molecules probed by regular Raman spectroscopy, respectively. I_{SERS} and I_{NR} correspond to the SERS intensity of p-ATP onto AgNPs surface and to the normal Raman scattering intensity of p-ATP in the bulk. I_{NR} and I_{SERS} were measured at 1078 cm^{-1}.

The crucial parameters for the quantitative analysis of the spectra are the laser spot area and the effective illuminated volume. The latter has been estimated using a formula recommended by Renishaw:

$$V = 3.21 \times \lambda^3 \left(\frac{f}{D}\right) \quad (4)$$

where f is the microscope objective focal length and D denotes the effective laser beam diameter at the objective back aperture. For our setup, $V = 2012 \approx 2 \times 10^3$ μm^3. The laser beam diameter, defined as twice the radius of a circle encompassing the area with 86% of the total power was about 5 μm; approximately the same values were obtained from the experimentally obtained laser spot image and from the theoretical formula ($4\lambda f/\pi D$). Assuming the volume in a shape of a cylinder with the diameter of 5 μm leads to the effective height of 100 μm. This value was confirmed by recording Raman spectra of Si while varying the distance from the focal plane.

The normal Raman spectrum was obtained for a cell filled with a pure p-ATP (125.19 g/mol) of density 1.17 g/cm^3. Under these conditions, $N_{NR} = 11.3 \times 10^{12}$ molecules were irradiated by the laser. The SERS samples were prepared by dipping AgNPs surface into diluted (9.0 mL of 1.0×10^{-6} M) solutions of p-ATP. The number of molecules contained in this solution was 5.4×10^{15}. The crucial point of this experiment is to ensure a less-than-a-monolayer coverage, otherwise the EF is overestimated. The surface of our samples was 20 mm^2. Assuming a surface of p-ATP of 42×10^{-8} μm^2 implies that the number of deposited molecules should not exceed 5×10^{13}. This is a very conservative estimate. In reality, the available surface is larger because of the substrate roughness. Anyway, we assured that the number of molecules probed by the laser beam (5 μm in diameter) is below that corresponding to the "flat" monolayer. The number of aminothiophenol molecules for the illuminated surface of 19.6 μm^2 was estimated as $N_{SERS} = 5.3 \times 10^6$. From these data of the relative intensity and the number of molecules sampled from the normal Raman and SERS measurements, the enhancement factor for four morphologically different surfaces were calculated and summarized in Table 1 with the particle density and size.

The highest EF of SERS intensity was obtained for p-ATP adsorbed on surface C (Figs. 2C and 3C). The EF in this case was several orders of magnitude larger than for the other morphologies (Table 1). The optimal morphology (sample C) corresponds to the highest coverage of the surface and the largest size of the silver particles (Table 1). A low EF value was obtained on the D surface with both lower surface coverage and AgNP size (Figs. 2D and 3D). We observed similar values of EF for surfaces A and B (Figs. 2A, 3A and 2B, 4b, respectively) with almost the same values of surface coverage but different particle sizes (the size of the AgNPs on surface B was two times greater than on surface A). Clearly the SERS intensity of adsorbates on the surface of metal nanoparticles depends on the interparticle distance and size of the nanoparticles [46].

Due to the highest Raman enhancement of surface C, resulting from the high Ag particle density (interparticle gap ~120 nm) and ~90 nm particle size, it was used for the rest of our SERS experiments.

3.4. Reproducibility of SERS spectra

For application purposes the SERS substrates should give reproducible spectra both across a single platform and between different platforms. Examples of a series of 4 vertically displaced SERS spectra of p-ATP adsorbed onto AgNPs films acquired at various positions on the same substrate and also on different substrates is shown in Fig. 4b. In each sampled region, the same modes appear with extremely high reproducibility with only a slight variation in amplitude for some of the higher wavenumber modes. The normalized second derivatives of the SERS spectra are shown in Fig. 4a. The almost complete overlap in features observed in the second derivative spectra indicate that the differences in the SERS spectra are primarily caused by total intensity and/or baseline variations and not due to variations in peak positions or in relative peak

Table 1
The enhancement factor (EF) for four morphologically different surfaces: A, B, C and D, presented in Fig. 2.

Sample	Figure	Surface coverage (%)	AgNPs size (nm)	EF
A	2A, 4a	30 ± 3	40 ± 17	1.2×10^3
B	2B, 4b	33 ± 2	76 ± 24	3.6×10^4
C	2C, 4c	47 ± 3	91 ± 43	1.8×10^7
D	2D, 4d	20 ± 1	33 ± 23	2.3×10^2

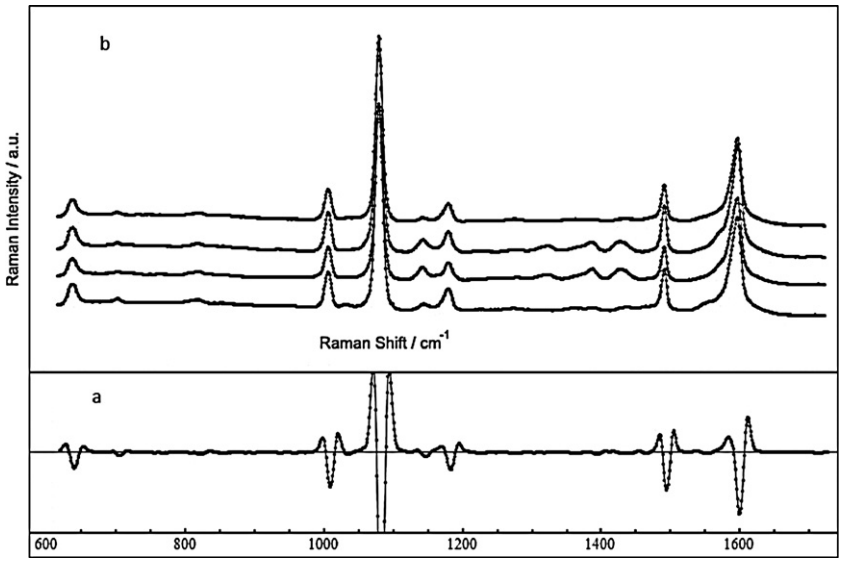

Fig. 4. SERS spectra of p-ATP from four different measurements (b), (a) second derivatives of the SERS spectra with calculated cross correlation coefficient Γ of 0.96. Laser = 632.8 nm, power = 5 mW, integration time = 10 s.

intensities. Γ was calculated as a cross-correlation between all pairs of spectra and the average Γ of 0.96 was obtained as a quantitative measure of the high degree of reproducibility observed.

We observed that our AgNP substrates always show better reproducibility compared to commercial substrates (Klarite). When developing SERS substrates one often has to compromise either on signal enhancement or on reproducibility and it is always challenging to have a SERS substrate with adequate signal enhancement and low intensity variation. Fig. 5 shows the comparison of p-ATP SERS spectra measured on a commercial substrate and on our AgNP substrates. We noticed that the signal enhancement from the commercial substrate was weak and three orders of magnitude lower than that of our AgNP substrate. The average correlation coefficient (Γ) of the signal intensity variation from the commercial substrate was in the range of 0.85–0.90, which is in good agreement with reported data [48]. Our AgNPs substrate showed better SERS performance with Γ as high as 0.96. The experiments were repeated for substrates from different batches and all of them show consistent results. The small intensity variation for our AgNPs substrates is remarkable and ranks among the best of results reported in the literature [27,32].

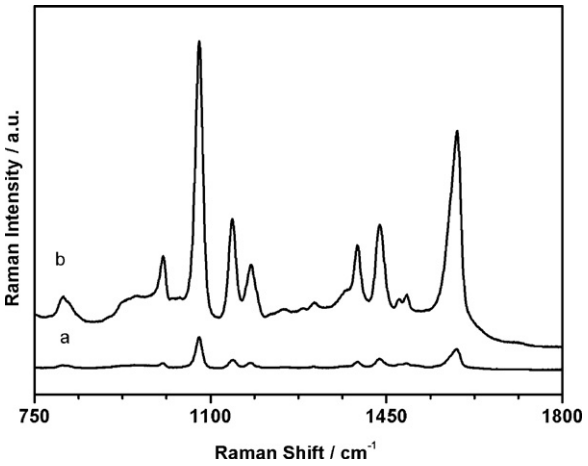

Fig. 5. Representation of the 10^{-6} M p-ATP SERS spectra from (a) commercial substrates and AgNPs substrate (b), before background subtraction. Laser = 632.8 nm, power = 5 mW, integration time = 90 s.

3.5. Stability of the surface

One of the principal objectives of the current study is to prepare SERS-active substrates that are suitable for biofluidic analysis. Since biofluids generally contain a certain amount of salts, it is important to study the stability of AgNPs surface in salt containing solutions. We measured the stability in aqueous solution containing 10% NaCl, which is about 10 times higher concentration than the normal physiological levels [43]. Typical UV–vis absorption spectra measured on these Ag films immersed in NaCl solution are shown in Fig. 6a. After a short time the spectra are generally identical, indicating that there is no appreciable morphological change in these films after the treatment. After 24 h of exposure to chlorine ions the signal decreases about 30%. This effect might be caused by AgCl deposit formation on the AgNPs. In the presence of nitrate no changes were observed (Fig. 6b).

Finally, we have to stress that our SERS-surfaces are physically and compositionally stable for an extended period of time. Fig. 7 illustrates SERS spectra of p-ATP recorded on a freshly prepared AgNP surface (Fig. 7a) and on a substrate stored for 3 months in ambient, light free conditions (Fig. 7b). These spectra showed that the SERS signal of p-ATP was reduced by only about 15% after 3 months on the shelf. The stability was higher still if the surface was stored in a refrigerator under N_2 atmosphere. This stability contrasts sharply with the commercially available SERS substrate where the spectral intensity decreases dramatically after only a few hours.

3.6. Neurotransmitters sensing

To examine the viability of the AgNP surface as a general SERS substrate for a variety of applications the biologically important neurotransmitters acetylcholine, dopamine, epinephrine and the acetylcholine precursor choline were tested. The detection and identification of neurotransmitters in brain fluid is an important problem in neurochemistry. Most important are measurements of concentration changes in correlation to neuronal events, i.e. measurements of the timescale of neuronal processes [49]. Commercially available SERS substrate like Klarite do not offer great enhancement for neurotransmitters. Fig. 8a–c shows SERS spectra of acetylcholine, dopamine and epinephrine adsorbed onto AgNPs substrates. SERS spectra of these three neurotransmitters

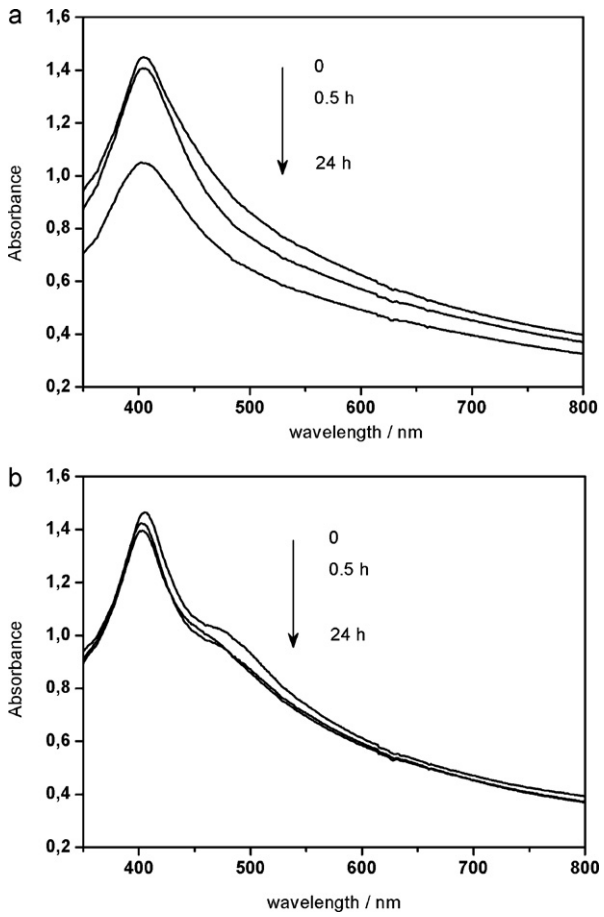

Fig. 6. UV–vis spectra of AgNP films in 10% of NaCl solution (a) and in 10% of KNO_3 solution (b) measured over time.

were measured at concentration of 7×10^{-4} M for epinephrine, 4×10^{-6} M for acetylcholine and 1×10^{-7} M for dopamine with accumulation times as short as 50 s. For acetylcholine [50] and dopamine [51] normal physiological concentration levels are expected to be in the same range. Fig. 9 depicts the normal Raman spectrum of choline in solution (Fig. 9a) and, for comparison, the SERS spectrum of choline adsorbed from 2.0×10^{-6} M water solution (Fig. 9b) which is a physiologically relevant concentration [52].

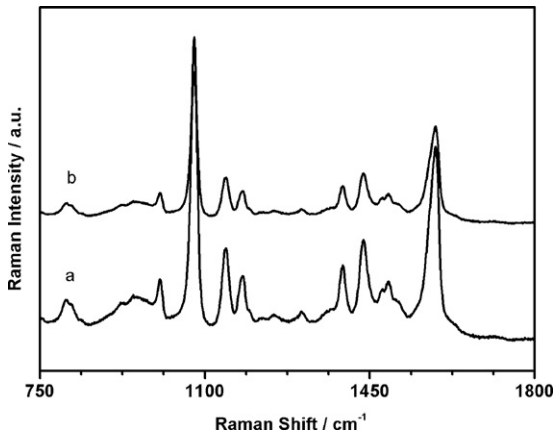

Fig. 7. SERS spectra of p-ATP recorded on a freshly prepared AgNPs surface (a) and on a AgNPs surface stored for 3 months under ambient conditions in air (b). Laser = 632.8 nm, power = 5 mW, integration time = 10 s.

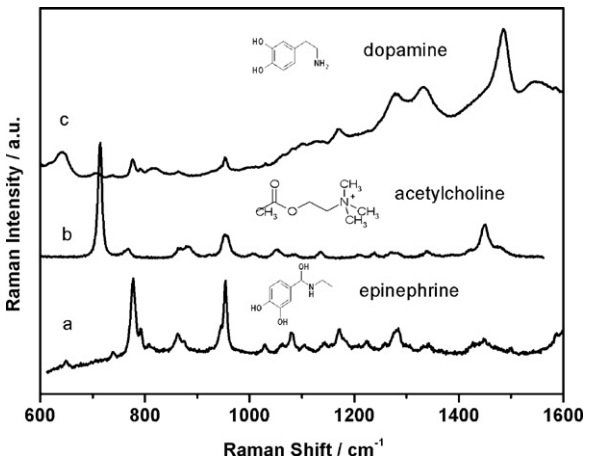

Fig. 8. SERS spectra of (a) epinephrine adsorbed onto AgNPs surface from 7×10^{-4} M aqueous solution, (b) acetylcholine adsorbed onto AgNPs surface from 4×10^{-6} M aqueous solution, (c) dopamine adsorbed onto AgNPs surface from its 1×10^{-7} M aqueous solution. Laser = 785 nm, power = 10 mW, integration time = 90 s.

The normal Raman and SERS spectra showed the same features with minor shifts of the frequencies of same bands. The strong band in the SERS spectrum at 714 cm^{-1} was assigned to the tetrahedrally symmetric N—C_4 stretching vibration. The band at 880 cm^{-1} corresponds to the totally symmetric N—$(CH_3)_3$ stretching vibration of the head group. All these bands are sensitive for the conformation of the molecule with respect to the C_α—C_β bond, and were observed at the frequencies that are characteristic for the gauche conformation [44]. Bands at 1132 cm^{-1} (weak), 1237 cm^{-1} (medium) and 1275 cm^{-1} (weak) are assigned to $\gamma(CH_3)$ rocking vibrations of the methyl groups in the positively charged head group. The remaining band at 1440 cm^{-1} (very strong) was attributed to symmetric deformational motions within the methyl groups.

We were not be able to detect any SERS spectra from Klarite substrate even for long accumulation times and from highly concentrated (1 M) solutions of neurotransmitters. Fig. 9c shows an example of the SERS spectrum of choline adsorbed from its 1 M aqueous solution collected for 15 min on Klarite. At the molar level only a very weak band at 723 cm^{-1} corresponding to the symmetric N—C_4 stretching vibration of choline is observed. By contrast, the SERS spectrum of choline on our AgNP substrate is intense at 10^{-6} M concentrations.

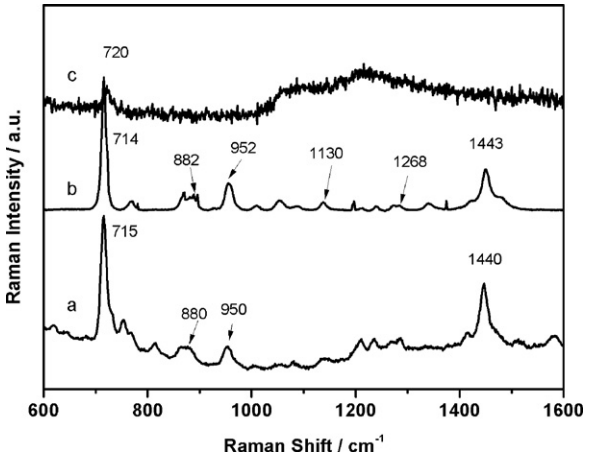

Fig. 9. (a) Normal Raman spectrum of 10^{-3} M aqueous solution of choline, (b) SERS spectrum of choline adsorbed from 2×10^{-6} M aqueous solution on AgNPs surface, and (c) choline onto Klarite adsorbed from 1 M solution. Laser = 785 nm, power = 10 mW, integration time = 90 s.

4. Conclusion

We fabricated SERS-active AgNP substrates by electrochemical deposition consistent with the principles of green chemistry. The size and surface coverage of the as-deposited AgNPs were controlled by changing the scan rate of the applied potential and the number of scans. The AgNP substrate exhibits SERS enhancements of up to 1.8×10^7 for p-aminothiophenol (p-ATP). This enhancement factor is three orders of magnitude larger than the corresponding one estimated for a commercial substrate used for comparison. The SERS enhancement was investigated as a function of the surface coverage and size of the AgNPs. The SERS study revealed excellent reproducibility of the AgNP substrate. The SERS spectra were the same for different spots on the same substrate and for different substrates obtained by our method. The substrate is stable over at least 3 months, whereas the commercial substrate does not show stability even after one day. We showed that our SERS substrate can be used to detect biological molecules such as neurotransmitters. High-quality SERS spectra at low concentrations and with short detection times were obtained for acetylcholine, dopamine and epinephrine. We also showed for the first time SERS of choline. The strong enhancement, reproducibility and stability of this AgNP substrate can be implemented in analysis systems for label-free chemical and biomolecular detection processes.

Acknowledgments

The work of A. Kaminska was realized within the POMOST Programme supported by the Foundation for Polish Science and co-financed by the EU "European Regional Development Fund" POMOST/2010–2/10 and through the grant "Iuventus Plus" (IP2010025970) by the Polish Ministry of Science and Higher Education. The work of J. Niedziolka-Jonsson was realized within the FOCUS Programme 3/2010 supported by the Foundation for Polish Science and partially supported by the National Centre for Research and Development within the LIDER Programme LIDER/15/24/L-2/10/NCBiR/2011.

References

[1] M. Fleischmann, P.J. Hendra, A.J. McQuillan, Raman spectra of pyridine adsorbed at a silver electrode, Chemical Physics Letters 26 (1974) 163.
[2] D.L. Jeanmaire, R.P. Van Duyne, Surface raman spectroelectrochemistry: Part I. Heterocyclic, aromatic, and aliphatic amines adsorbed on the anodized silver electrode, Journal of electroanalytical chemistry and interfacial electrochemistry 84 (1977) 1.
[3] K. Kneipp, H. Kneipp, I. Itzkan, R. Dasari, M. Feld, Ultrasensitive Chemical Analysis By Raman Spectroscopy, Chemical Review 99 (1999) 2957.
[4] S.J. Oldenburg, R.D. Averitt, S.L. Westcott, N.J. Halas, Nanoengineering of optical resonances, Chemical Physics Letters 288 (1988) 243.
[5] J. Aizpurua, P. Hanarp, D.S. Sutherland, M. Käll, G.W. Bryant, F.J. Garcia de Abajo, Optical Properties of Gold Nanorings, Physical Review Letters 90 (2003) 057401.
[6] P. Freunscht, R.P. Van Duyne, S. Schneider, Surface-enhanced Raman spectroscopy of trans-stilbene adsorbed on platinum- or self-assembled monolayer-modified silver film over nanosphere surfaces, Chemical Physics Letters 281 (1997) 372.
[7] C. McLaughlin, D. Graham, W.E. Smith, Comparison of Resonant and Non Resonant Conditions on the Concentration Dependence of Surface Enhanced Raman Scattering from a Dye Adsorbed on Silver Colloid, The Journal of Physical Chemistry B 106 (2002) 5408.
[8] B. Nikoobakht, J. Wang, M.A. El-Sayed, Surface-enhanced Raman scattering of molecules adsorbed on gold nanorods: off-surface plasmon resonance condition, Chemical Physics Letters 366 (2002) 17.
[9] M. Rycenga, C.M. Cobley, J. Zeng, W. Li, C.H. Moran, Q. Zhang, D. Qin, Y. Xia, Controlling the Synthesis and Assembly of Silver Nanostructures for Plasmonic Applications, Chemical Reviews 111 (2011) 3669.
[10] D.P. Tsai, J. Kovacs, Z. Wang, M. Moskovits, V.M. Shalaev, J.S. Suh, R. Botet, Photon scanning tunneling microscopy images of optical excitations of fractal metal colloid clusters, Physical Review Letters 72 (1994) 4149.
[11] M.A. El-Sayed, Some Interesting Properties of Metals Confined in Time and Nanometer, Space of Different Shapes, Accounts of Chemical Research 34 (2001) 257.
[12] M. Fan, G.F.S. Andrade, A.G. Brolo, A review on the fabrication of substrates for surface enhanced Raman spectroscopy and their applications in analytical chemistry, Analytica Chimica Acta 693 (2011) 7.
[13] A. Campion, P. Kambhampati, Surface-enhanced Raman scattering, Chemical Society Reviews 27 (1998) 241.
[14] M. Cardona, G. Guntherodt, A. Otto, Surface-enhanced Raman scattering: "Classical" and "Chemical" origins, in: M. Cardona, G. Guntherodt (Eds.), Light Scattering in Solids IV, vol. 54, Springer, Berlin Heidelberg, 1984, pp. 289.
[15] F.R. Aussenegg, M.E. Lippitsch, On raman scattering in molecular complexes involving charge transfer, Chemical Physics Letters 59 (1978) 214.
[16] V.M. Shalaev, A.K. Sarychev, Nonlinear optics of random metal-dielectric films, Physical Review B 57 (1998) 13265.
[17] K. Kneipp, Y. Wang, H. Kneipp, L.T. Perelman, I. Itzkan, R.R. Dasari, M.S. Feld, Single Molecule Detection Using Surface-Enhanced Raman Scattering (SERS), Physical Review Letters 78 (1997) 1667.
[18] K. Kneipp, H. Kneipp, M.S. Dresselhaus, S. Lefrant, Surface-enhanced Raman scattering on single-wall carbon nanotubes, Philosophical Transactions of the Royal Society of London. Series A: mathematical, Physical and Engineering Sciences 362 (2004) 2361.
[19] S. Nie, S.R. Emory, Probing Single Molecules And Single Nanoparticles By Surface-Enhanced Raman Scattering, Science 275 (1997) 1102.
[20] S. Zou, G.C. Schatz, Silver nanoparticle array structures that produce giant enhancements in electromagnetic fields, Chemical Physics Letters 403 (2005) 62.
[21] M.E. Hankus, H. Li, G.J. Gibson, B.M. Cullum, Surface-Enhanced Raman Scattering-Based Nanoprobe for High-Resolution, Non-Scanning Chemical Imaging, Analytical Chemistry 78 (2006) 7535.
[22] M.A. De Jesús, K.S. Giesfeldt, J.M. Oran, N.A. Abu-Hatab, N.V. Lavrik, M.J. Sepaniak, Nanofabrication of Densely Packed Metal-Polymer Arrays for Surface-Enhanced Raman Spectrometry, Applied Spectroscopy 59 (2005) 1501.
[23] J.D. Driskell, S. Shanmukh, Y. Liu, S.B. Chaney, X.J. Tang, Y.P. Zhao, R.A. Dluhy, The Use of Aligned Silver Nanorod Arrays Prepared by Oblique Angle Deposition as Surface Enhanced Raman Scattering Substrates, The Journal of Physical Chemistry C 112 (2008) 895.
[24] M.A. Khan, T.P. Hogan, B. Shanker, Gold-coated zinc oxide nanowire-based substrate for surface-enhanced Raman spectroscopy, Journal of Raman Spectroscopy 40 (2009) 1539.
[25] S.P. Mulvaney, L. He, M.J. Natan, C.D. Keating, Three-layer substrates for surface-enhanced Raman scattering: preparation and preliminary evaluation, Journal of Raman Spectroscopy 34 (2003) 163.
[26] J.M. Oran, R.J. Hinde, N. Abu Hatab, S.T. Retterer, M.J. Sepaniak, Nanofabricated periodic arrays of silver elliptical discs as SERS substrates, Journal of Raman Spectroscopy 39 (2008) 1811.
[27] L.-L. Qu, D.-W. Li, J.-Q. Xue, W.-L. Zhai, J.S. Fossey, Y.-T. Long, Batch fabrication of disposable screen printed SERS arrays, Lab on a Chip 12 (2012) 876.
[28] E. Galopin, A. Noual, J. Niedziolka-Jonsson, M. Jonsson-Niedziolka, A. Akjouj, Y. Pennec, B. Djafari-Rouhani, R. Boukherroub, S. Szunerits, Short- and Long-Range Sensing Using Plasmonic Nanostrucures: experimental and Theoretical Studies, The Journal of Physical Chemistry C 113 (2009) 15921.
[29] C. Zhu, G. Meng, Q. Huang, Z. Zhang, Q. Xu, G. Liu, Z. Huang, Z. Chu, Ag nanosheet-assembled micro-hemispheres as effective SERS substrates, Chemical Communications 47 (2011) 2709.
[30] C. Zhu, G. Meng, Q. Huang, Z. Li, Z. Huang, M. Wang, J. Yuan, Large-scale well-separated Ag nanosheet-assembled micro-hemispheres modified with HS-β-CD as effective SERS substrates for trace detection of PCBs, Journal of Materials Chemistry 22 (2012) 2271.
[31] J.-C. Bian, Z. Li, Z.-D. Chen, H.-Y. He, X.-W. Zhang, X. Li, G.-R. Han, Electrodeposition of silver nanoparticle arrays on ITO coated glass and their application as reproducible surface-enhanced Raman scattering substrate, Applied Surface Science 258 (2011) 1831.
[32] J. Bian, Z. Li, Z. Chen, X. Zhang, Q. Li, S. Jiang, J. He, G. Han, Double-potentiostatic electrodeposition of Ag nanoflowers on ITO glass for reproducible surface-enhanced (resonance) Raman scattering application, Electrochimica Acta 67 (2012) 12.
[33] G.H. Gu, J.S. Suh, Hexagonally Patterned Silver Nanoparticles Electrodeposited on an Aluminum Plate for Surface-Enhanced Raman Scattering, The Journal of Physical Chemistry C 114 (2010) 7258.
[34] G.H. Gu, J. Kim, L. Kim, J.S. Suh, Optimum Length of Silver Nanorods for Fabrication of Hot Spots, The Journal of Physical Chemistry C 111 (2007) 7906.
[35] E. Gomez, J. Garcia-Torres, E. Valles, Study and preparation of silver electrodeposits at negative potentials, Journal of Electroanalytical Chemistry 594 (2006) 89.
[36] W. Plieth, H. Dietz, A. Anders, G. Sandmann, A. Meixner, M. Weber, H. Kneppe, Electrochemical preparation of silver and gold nanoparticles: characterization by confocal and surface enhanced Raman microscopy, Surface Science 597 (2005) 119.
[37] M. Muniz-Miranda, B. Pergolese, A. Bigotto, A. Giusti, Stable and efficient silver substrates for SERS spectroscopy, Journal of Colloid and Interface Science 314 (2007) 540.
[38] O. Arias-Carrion, E. Poppel, Dopamine, learning, and reward-seeking behavior, Acta Neurobiologiae Experimentalis 67 (2007) 481.

[39] K. Kneipp, H. Kneipp, I. Itzkan, R.R. Dasari, M.S. Feld, Surface-enhanced Raman scattering and biophysics, Journal of Physics: condensed Matter 14 (2002) R597.
[40] N.S. Lee, Y.Z. Hsieh, R.F. Paisley, M.D. Morris, Surface-enhanced Raman spectroscopy of the catecholamine neurotransmitters and related compounds, Analytical Chemistry 60 (1988) 442.
[41] M.L. McGlashen, K.L. Davis, M.D. Morris, Surface-enhanced Raman scattering of dopamine at polymer-coated silver electrodes, Analytical Chemistry 62 (1990) 846.
[42] F. Wei, D. Zhang, N.J. Halas, J.D. Hartgerink, Aromatic Amino Acids Providing Characteristic Motifs in the Raman and SERS Spectroscopy of Peptides, The Journal of Physical Chemistry B 112 (2008) 9158.
[43] N.M.B. Perney, F.J. Garcia de Abajo, J.J. Baumberg, A. Tang, M.C. Netti, M.D.B. Charlton, M.E. Zoorob, Tuning localized plasmon cavities for optimized surface-enhanced Raman scattering, Physical Review B 76 (2007) 035426.
[44] C.D. Chen, S.F. Cheng, L.K. Chau, C.R.C. Wang, Successively amplified electrochemical immunoassay based on biocatalytic deposition of silver nanoparticles and silver enhancement, Biosensors & Bioelectronics 22 (2007) 926.
[45] K.G. Stamplecoskie, J.C. Scaiano, Light Emitting Diode Irradiation Can Control the Morphology and Optical Properties of Silver Nanoparticles, Journal of the American Chemical Society 132 (2010) 1825.
[46] M. Osawa, N. Matsuda, K. Yoshii, I. Uchida, Charge transfer resonance Raman process in surface-enhanced Raman scattering from p-aminothiophenol adsorbed on silver: Herzberg-Teller contribution, The Journal of Physical Chemistry 98 (1994) 12702.
[47] K. Kim, J.K. Yoon, Raman Scattering of 4-Aminobenzenethiol Sandwiched between Ag/Au Nanoparticle and Macroscopically Smooth Au Substrate, The Journal of Physical Chemistry B 109 (2005) 20731.
[48] B. Nowicki, Multiparameter representation of surface roughness, Wear 102 (1985) 161.
[49] B.H.C. Westerink, G. Damsma, H. Rollema, J.B. De Vries, A.S. Horn, Scope and limitations of in vivo brain dialysis: a comparison of its application to various neurotransmitter systems, Life Sciences 41 (1987) 1763.
[50] M. Watanabe, A. Kimura, K. Akasaka, S. Hayashi, Determination of acetylcholine in human blood, Biochemical Medicine and Metabolic Biology 36 (1986) 355.
[51] S. Ali, R. Parajuli, Y. Balogun, Y. Ma, H. He, A Nonoxidative Electrochemical Sensor Based on a Self-Doped Polyaniline/Carbon Nanotube Composite for Sensitive and Selective Detection of the Neurotransmitter Dopamine: a Review, Sensors 8 (2008) 8423.
[52] S.H. Zeisel, Choline: an essential nutrient for humans, Nutrition 16 (2000) 669.